Reversible Valence Equilibrium Reactions in Main Group Compounds. A Theoretical Study

Meng-Lin Tsai and Ming-Der Su*

Department of Applied Chemistry, National Chiayi University, Chiayi 60004, Taiwan

Received: January 19, 2006; In Final Form: March 24, 2006

The potential energy surface for the intramolecular reaction of singlet state RR′E═ERR′ (E = C, Si, Ge, Sn, and Pb) has been explored using density functional theory. All the stationary points, including the unsymmetrical reactant ($R'R_2E-ER'$), the transition state, the symmetric product (R′RE═ERR′), and the monomer (R′RE) were completely optimized at the B3LYP/LANL2DZdp level of theory. Our theoretical findings suggest the following: (1) Both double-bonded RR′C═CRR′ and RR′Si═SiRR′ species are true minima on their potential energy surfaces and should be the only compounds existing at all temperatures. (2) The germanium system will occur either in the dimeric $R_2R'Ge-GeR'$ and RR′Ge═GeRR′ structures or the monomeric RR′Ge structure, depending on the temperature. (3) If the size of the substituent (R) is small, then the unsymmetrical single-bonded $R_2R'Sn-SnR'$ molecule can exist at low temperatures. At room temperature, the unsymmetrical $R_2R'Sn-SnR'$ species can exist in equilibrium with its RR′Sn monomer. (4) The unsymmetrical $R_3Pb-PbR$ compound may be kinetically stable at low temperatures. On the other hand, it is predicted that both the unsymmetrical $R_3Pb-PbR$ and the symmetric $R_2Pb═PbR_2$ species will spontaneously dissociate into R_2Pb monomers at room temperature. Our theoretical results are in good agreement with available experimental observations (*J. Am. Chem. Soc.* **2003**, *125*, 7520), and the results obtained allow a number of predictions to be made.

I. Introduction

Recent studies concerning the chemistry of double-bonded compounds of the heavier group 14 elements have demonstrated that they are not fictitious and have real existence as stable compounds.[1,2] Even tin[3] and lead[4] have been shown to form such compounds when they are sufficiently kinetically stabilized. Indeed, there have been a growing number of reviews[5] reflecting the large scientific activity in this area.

Currently, there is widespread interest in the reactivity of these fascinating double-bonded systems. However, research in the field of the heavier alkenes, E = Sn or Pb, is hampered by the relative weakness of the E═E double bonds, and it is often necessary to work at low temperatures in an inert atmosphere and to use sterically protecting substituents.[3,4] Theoretical studies on the hypothetical hydrogen derivatives E_2H_4 show that the doubly bridged *trans*-$HE(\mu\text{-}H)_2EH$ (**I**) is more stable than the unsymmetrical structure H_3E-EH (**II**), but that the latter is more stable than the trans-bent symmetric structure $H_2E═EH_2$ (**III**) for E = Sn, Pb, but not for E = Si, Ge.[6] Besides these, the energy differences between the unsymmetrical (**II**) and trans-bent symmetric (**III**) forms were predicted to be less than 10 kcal/mol for E = Sn and Pb. However, the lower bridging tendency of a bulky group (R)[7] suggests that the bridging structure in *trans*-$RE(\mu\text{-}R)_2ER$ (**I**) may not be the most stable, and that the R_3E-ER (**II**) isomer may be the preferred one in the hypothetical E_2R_4 species. However, to the best of our knowledge, this has not been verified by any theoretical calculations (vide infra).

Recently, through the elegant studies performed by Power and co-workers,[8] it was found that the addition of LiPh to Ar*SnCl (Ar* = C_6H_3-2,6-$Trip_2$; Trip = $C_6H_2-2,4,6\text{-}{}^iPr_3$) at a

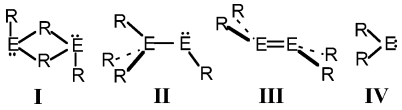

I **II** **III** **IV**

moderately low temperature produced the Sn(III)−Sn(I) species $Ar^*Ph_2SnSnAr^*$. As demonstrated in Scheme 1, the ^{119}Sn NMR spectrum displays two signals (δ = 246 and 2857 ppm) at −60°, which is consistent with the unsymmetrical structure $Ar^*Ph_2Sn-SnAr^*$ (**II**). Finally, as the temperature is raised, these two signals disappear and only a single broad resonance near δ = 1517 ppm is observed. The chemical shift for the high-temperature spectrum establishes the presence of two-coordinated Ar*−Sn−Ph in solution.[8] These spectra are thus in agreement with an equilibrium given by

$$Ar^*Ph_2Sn-SnAr^* \rightleftarrows Ar^*-Sn-Ph \qquad (1)$$

This may be contrasted with the situation of germanium and lead where the symmetric dimer Ar*PhGe═GePhAr*[9] and monomer Ar*−Pb−Ph[10] (**IV**) were obtained exclusively upon reaction of Ar*GeCl or Ar*PbBr with LiPh. On the other hand, all currently known compounds R_2SnSnR_2 and R_2PbPbR_2, as well as many R_2GeGeR_2 species, have E═E bonded dimeric structures in the solid state, but dissociate in solution to yield the monomers: R_2E (**IV**; E = Ge, Sn, or Pb). That is, a dimer-monomer equilibrium in solution given by

$$R_2E═ER_2 \rightleftarrows 2R_2E \qquad (2)$$

(E = Ge, Sn, and Pb; R = large organic ligand)

can exist.[11] Moreover, these experimental findings strongly indicate that the bonding between these elements is relatively weak.[5g,12]

* To whom correspondence should be addressed. E-mail: midesu@mail.ncyu.edu.tw.

10.1021/jp060396m CCC: $33.50
Published on Web 04/27/2006

SCHEME 1

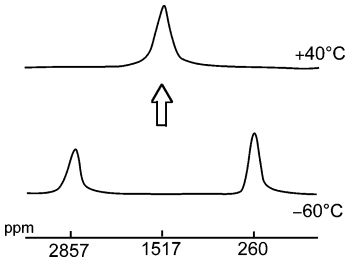

It is this fascinating experimental progress that has inspired this study. As far as we are aware, no theoretical study of such equilibrium reactions involving the heavier main group compounds has been reported, even though the reactions of eq 2 are well-known experimentally. Since the dimer−monomer equilibrium reactions are both novel and useful, their detailed mechanistic knowledge would facilitate a more pronounced control of their reactivity.

In this work we present the first density functional theory (DFT) study of the $E_2Ar'_2Ph_2$ ($Ar' = C_6H_3$-1,5-$(CH_3)_2$)[13] potential surfaces, with E varying from carbon to lead. The existence, as true minima, of the unsymmetrical structure (**II**) and the trans-bent double bond (**III**) as well as the two-coordinated monomer (**IV**) and their relative energies are the main points of concern. Consequently, we propose a possible mechanism for the equilibrium process demonstrated in eq 3: in the first stage, the unsymmetrical $Ar'Ph_2E-EAr'$ molecule undergoes a 1,2-Ph migration which results in the formation of a symmetric Ar′PhE═EPhAr′ structure. This double-bonded species then dissociates to form two V-shaped monomers, Ar′PhE.

$$Ar'Ph_2E-EAr'\ (\mathbf{II}) \rightarrow TS \rightarrow Ar'PhE{=}EPhAr'\ (\mathbf{III}) \rightarrow 2Ar'PhE\ (\mathbf{IV})$$
$$(E = C, Si, Ge, Sn, \text{and } Pb) \qquad (3)$$

ΔG potential energy surfaces of reaction 3 are presented and discussed, which should be useful for the interpretations of the future experimental observations. In fact, it is believed that, in view of recent dramatic developments in main group chemistry,[1−5] analogous extensive studies of the equilibria of compounds involving main group elements in different oxidation states should soon be forthcoming and open up new areas.

II. Calculation Methods

All geometries were fully optimized without imposing any symmetry constraints, although several optimized structures showed various elements of symmetry. For our DFT calculations, we used the hybrid gradient-corrected exchange functional proposed by Becke,[14] combined with the gradient-corrected correlation functional of Lee, Yang, and Parr.[15] Thus, the geometries of all the stationary points were fully optimized at the B3LYP level of theory. These B3LYP calculations were carried out with pseudo-relativistic effective core potentials on group 14 elements modeled using the double-ζ (DZ) basis sets[16] augmented by a set of d-type polarization functions.[17] The DZ basis set for the hydrogen element was augmented by a set of p-type polarization functions (p exponents 0.356). The d exponents used for C, Si, Ge, Sn, and Pb are 0.587, 0.296, 0.246, 0.186, and 0.179, respectively. Accordingly, we denote our B3LYP calculations by B3LYP/LANL2DZdp. It is noted that the model compounds Ar′PhEEPhAr′ and Ar′PhE have 676 (204 electrons) and 338 (102 electrons) basis functions for E = C, Si, Ge, Sn, and Pb. The spin-unrestricted (UB3LYP) formalism was used for the open-shell (triplet) species. The computed expectation values of the spin-squared operator $\langle S^2 \rangle$ were in the range of 2.001−2.012 for all triplet species considered here, and they were therefore very close to the correct value of 2.0 for pure triplets, so that their geometries and energetics are reliable for this study.

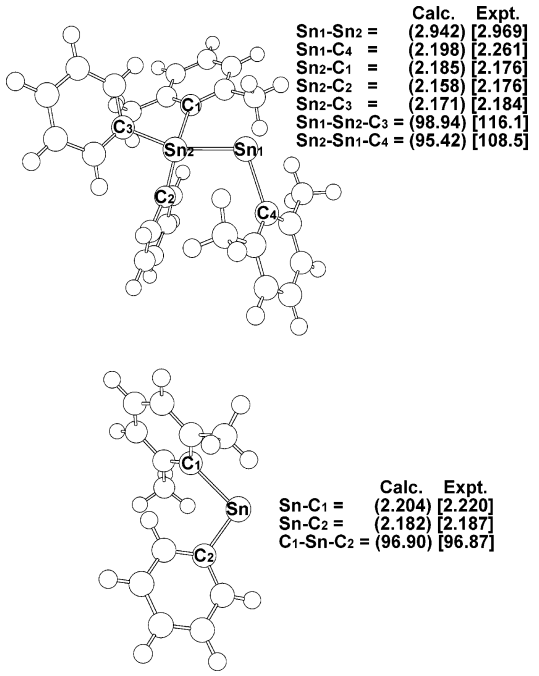

Figure 1. Comparison of B3LYP/LANL2DZdp optimized geometries and experimental values (in Å and deg). See text.

Frequency calculations were performed on all structures to confirm that the reactants and products had no imaginary frequencies, and that transition states (TSs) possessed only one imaginary frequency. The relative energies at 0 K were thus corrected for vibrational zero-point energies (ZPE, not scaled). Thermodynamic corrections to 298 K, ZPE corrections, heat capacity corrections, and entropy corrections (ΔS) obtained were applied at the B3LYP/LANL2DZdp level. Thus, the relative free energy (ΔG) at 298 K was also calculated at the same level of theory. All of the DFT calculations were performed using the GAUSSIAN 03 package of programs.[18]

III. Results and Discussion

Before discussing the potential energy surfaces for the equilibrium reactions (eq 3), we shall first discuss the geometries of the unsymmetrical reactant (**II**) and the two-coordinated product (**IV**). Unfortunately, as mentioned in the Introduction, only one stable unsymmetrical compound (**II**) with a Sn−Sn single bond has been isolated and characterized unequivocally, i.e., $Ar^*Ph_2Sn-SnAr^*$ by Power and co-workers.[8,19] Selected geometric parameters for the experimentally observed $Ar^*Ph_2Sn-SnAr^*$ and Ar*−Sn−Ph molecules are given in Figure 1, along with the corresponding values calculated for the $Ar'Ph_2Sn-SnAr'$ and Ar′−Sn−Ph model compounds. As one can see in Figure 1, in principle, our DFT results for the structure of $Ar'Ph_2Sn-SnAr'$ are in reasonable agreement with the available experimental data for that of $Ar^*Ph_2Sn-SnAr^*$. For instance, the Sn−Sn bond length determined by X-ray diffraction for $Ar^*Ph_2Sn-SnAr^*$ is 2.969 Å,[8] while our predicted B3LYP bond length for $Ar'Ph_2Sn-SnAr'$ is 2.942 Å. In addition, the Sn−C bond lengths in $Ar^*Ph_2Sn-SnAr^*$ (2.261−2.176 Å)[8] are

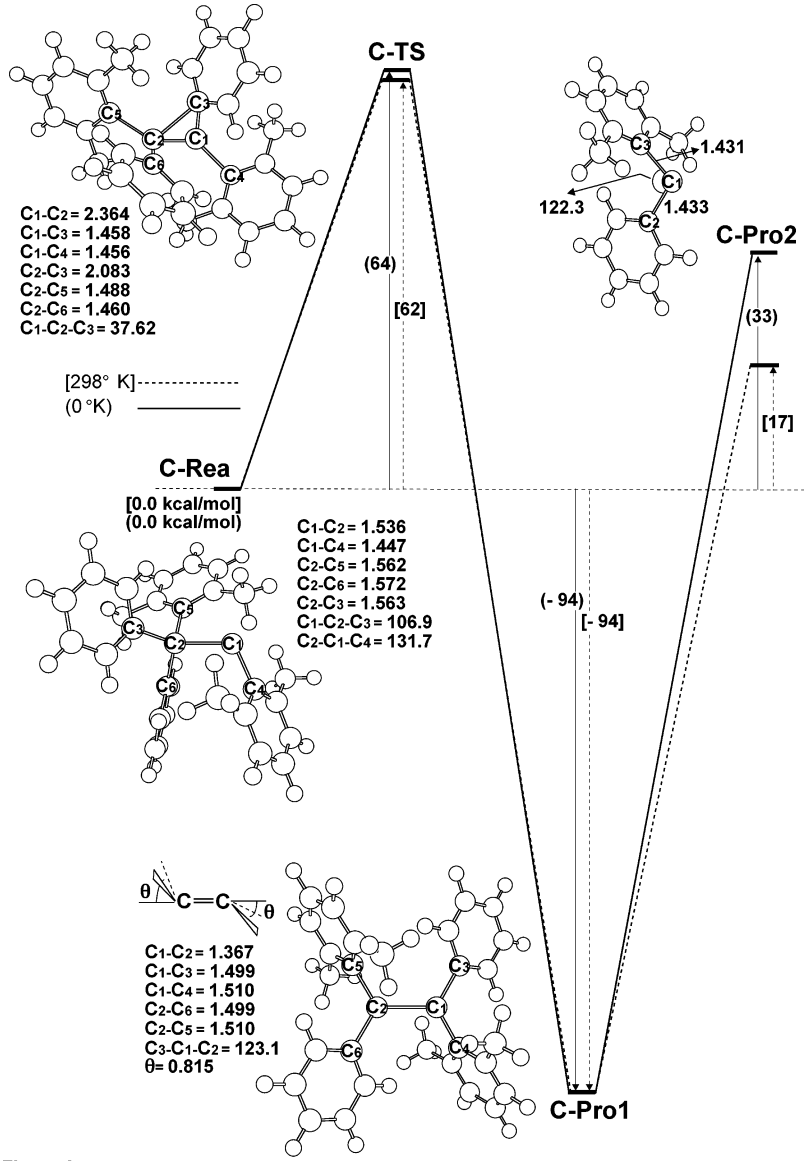

Figure 2. B3LYP/LANL2DZdp optimized geometries (in Å and deg) and relative energies of ArPh2C·CAr (C·Rea), transition state (C·TS), ArPhC═CPhAr (C·Pro1), and ArPhC (C·Pro2) at 0 and 298 K.

somewhat larger than those in the Ar′Ph_2Sn−SnAr′ structure (2.198−2.158 Å), bearing in mind that the synthesized molecule contains bulkier substituents. Similarly, Figure 1 shows a wider bond angle (∠Sn_2−Sn_1−C_4) of 108.5° in Ar*Ph_2Sn−SnAr*, whereas a narrow bond angle of 95.42° is found in Ar′Ph_2Sn−SnAr′. This phenomenon can also be found in other bond angles of Ar*Ph_2Sn−SnAr* and Ar′Ph_2Sn−SnAr′ as shown in Figure 1. These wider angles in the former molecule are somewhat surprising and are presumably due to the large size of the bulky terphenyl group.

In addition, one may compare the structural parameters of the V-shaped Ar*−Sn−Ph and Ar′−Sn−Ph (**IV**) as given in Figure 1. The agreement between both bond lengths and bond angles in Ar*−Sn−Ph and Ar′−Sn−Ph is quite good, with the bond lengths and angles in agreement to within 0.005 Å and 0.03°, respectively. In any event, the good agreement between our computational results and the available experimental data is encouraging. We therefore believe that the present models with the current method (B3LYP/LANL2DZdp) employed in this study should provide reliable information for the discussion of the reaction mechanism, for which experimental data are still not available.

Selected geometrical parameters for the stationary point structures along the pathway given in eq 3 calculated at the B3LYP/LANL2DZdp level are shown in Figures 2−6 for E = C, Si, Ge, Sn, and Pb, respectively. The relative energies obtained at the same level of theory are collected in Table 1. Cartesian coordinates for these stationary points are included in the Supporting Information. Several noteworthy features from Figures 2−6 and Table 1 are revealed.

1. The Ar′Ph_2E═EAr′ (E = C, Si, Ge, Sn, and Pb) Reactant. Let us first discuss the reactant −the unsymmetrical Ar′Ph_2E−EAr′ (**II**) species. The five sets of unsymmetrical reactants used in the present work are shown in Figures 2−6: **C−Rea** (Ar′Ph_2C−CAr′), **Si−Rea** (Ar′Ph_2Si−SiAr′), **Ge−Rea** (Ar′Ph_2Ge−GeAr′), **Sn−Rea** (Ar′Ph_2Sn−SnAr′), and **Pb−Rea** (Ar′Ph_2Pb−PbAr′), respectively. Of these, as stated earlier, only **Sn−Rea**[8,19] has been generated as a stable compound, in which the tin atoms have different substituents and different formal oxidation states, i.e., Sn(III)−Sn(I).

According to our DFT frequency calculations, these unsymmetrical Ar′Ph_2E−EAr′ (**II**) reactants have no imaginary frequency and are true minima on the potential energy surfaces.[20,21] In addition, our B3LYP/LANL2DZdp results indicate

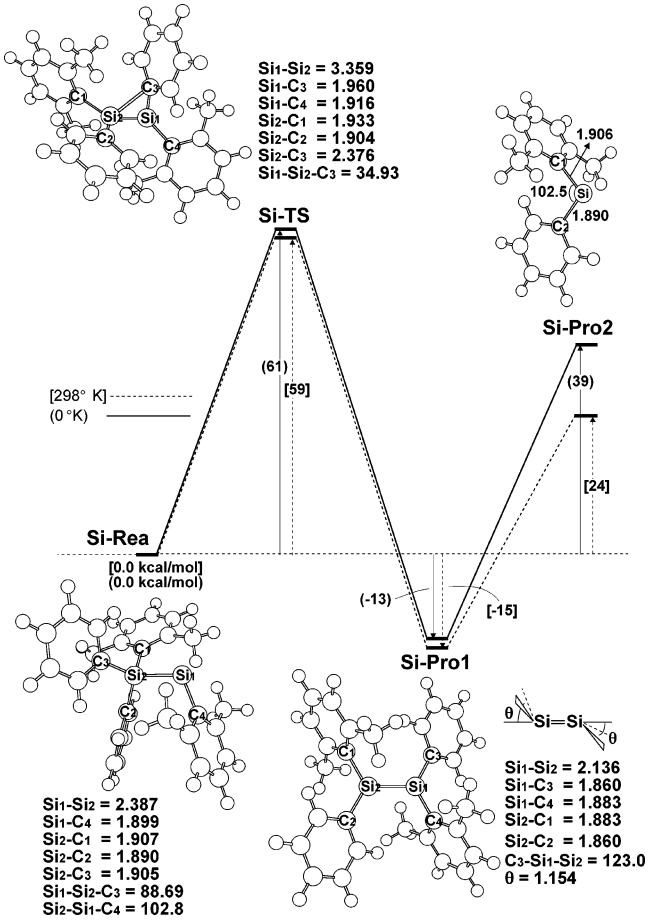

Figure 3. B3LYP/LANL2DZdp optimized geometries (in Å and deg) and relative energies of ArPh2Si·SiAr (Si·Rea), transition state (Si·TS), ArPhSi═SiPhAr (Si·Pro1), and ArPhSi (Si·Pro2) at 0 and 298 K.

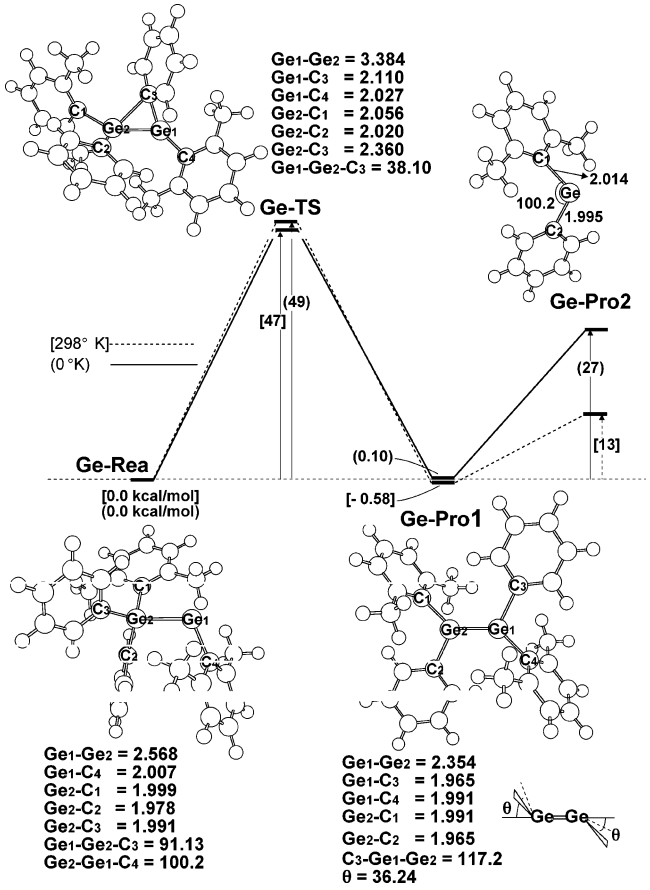

Figure 4. B3LYP/LANL2DZdp optimized geometries (in Å and deg) and relative energies of ArPh2Ge·GeAr (Ge.Rea), transition state (Ge·TS), ArPhGe═GePhAr (Ge·Pro1), and ArPhGe (Ge·Pro2) at 0 and 298 K.

that all of the unsymmetrical species studied in this work, which are analogous to substituted heavy carbenes, are singlets in their ground state. As often observed,[22] the stability of the singlet state increases with decreasing electronegativity at the central atom E in Ar′Ph_2E−EAr′ (**II**). That is to say, the singlet−triplet energy splitting ($\Delta E_{st} = E_{triplet} - E_{singlet}$) generally increases as the atomic number of the central atom E is increased. The reason for this may be due partially to the fact that the relativistic effect[22] on a heavier central atom stabilizes the s orbital relative to the p orbital, favoring the singlet state relative to the triplet. This prediction is confirmed by our theoretical results, i.e., an increasing trend in ΔE_{st} for **C**−**Rea** (0.13 kcal/mol) < **Si**−**Rea** (25 kcal/mol) < **Ge**−**Rea** (27 kcal/mol) < **Sn**−**Rea** (28 kcal/mol) < **Pb**−**Rea** (34 kcal/mol) at the B3LYP/LANL2DZdp level of theory. Consequently, it is reasonable to conclude that the equilibrium reactions (eq 3) should proceed on the singlet surface. We shall thus focus on this singlet surface from now on.

Moreover, the computational results presented in Figures 2−6 demonstrate that the calculated E−E single bond lengths in Ar′Ph_2E−EAr′ (**II**) increase in the order 1.536 Å (**C**−**Rea**) < 2.387 Å (**Si**−**Rea**) < 2.568 Å (**Ge**−**Rea**) < 2.942 Å (**Sn**−**Rea**) < 3.022 Å (**Pb**−**Rea**). Namely, heavy main group 14 element substitution causes a large increase in the E−E bond length of Ar′Ph_2E−EAr′. This finding can be explained in terms of the expected atomic size of the central atom E, which increases as E changes from C to Pb. Likewise, as seen in Figures 2−6, the $\angle E_2-E_1-C_4$ bond angles (where E_1 is the heavy carbene center) follows the inverse trend as the E−E bond length, i.e., 132° (**C**−**Rea**) > 103° (**Si**−**Rea**) > 100° (**Ge**−**Rea**) > 95.4° (**Sn**−**Rea**) > 95.0° (**Pb**−**Rea**).[23] Moreover, it appears that, as the E atom becomes heavier, an $\angle E_2-E_1-C_4$ bond angle approaching 90° is preferred. Again, the reason for this may be due to the relativistic effect.[24] As E changes from carbon to lead, the valence s orbital is more strongly contracted than the corresponding p orbitals.[24(b)] Namely, the size difference between the valence s and p orbitals increases from C to Pb (the significant 6s orbital contraction originates mostly from the relativistic effect). Consequently, the valence s and p orbitals differ in spatial extension and overlap less to form strong hybrid orbitals.[24] In other words, the so-called "inert s-pair effect" (or "nonhybridization effect")[24] occurs on moving from silicon to lead. As a result, the preference for a bond angle $\angle E_2-E_1-C_4$ approaching 90° is a consequence of the decreased hybridization of the s and p orbitals in the heavier main group 14 elements. In the case of tin and lead, hybridization is further diminished by the relativistic effect.[24]

Furthermore, it is likely in general that an unsymmetrical R_3E-ER structure similar to **II** will be energetically less stable than a symmetric $R_2E{=}ER_2$ structure similar to **III**, owing to the steric conflict between the three large *R* groups attached to the same atom in **II**. However, it was found experimentally that, for tin, the C_6H_3-2,6-$Trip_2$ (Ar*) substituent mentioned earlier allows structure **II** to be isolated with small groups as co-ligands.[8,19] The reasons for the unexpected preference of a RR'_2-Sn−SnR (**II**) over a RR′Sn═SnRR′ (**III**) structure may be due, as suggested by Power et al.,[8,9,19] to the relative weakness of the Sn═Sn double bond[11d,25] and the small size of the organic substituents (R′; such as the phenyl group in this work) that would not unduly crowd the tin environment. Indeed, as seen

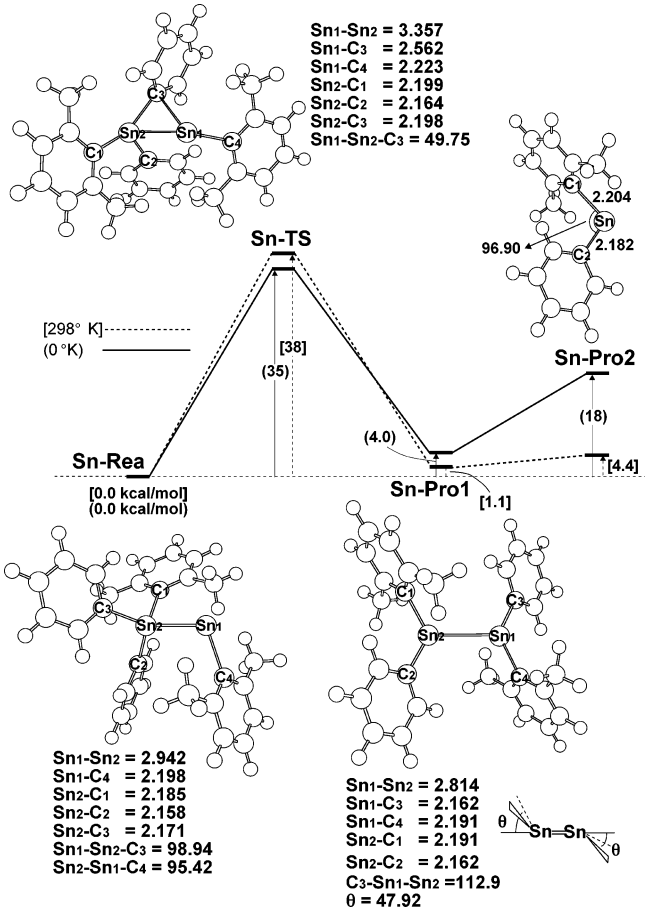

Figure 5. B3LYP/LANL2DZdp optimized geometries (in Å and deg) and relative energies of ArPh2Sn·SnAr (Sn·Rea), transition state (Sn·TS), ArPhSn═SnPhAr (Sn·Pro1), and ArPhSn (Sn·Pro2) at 0 and 298 K.

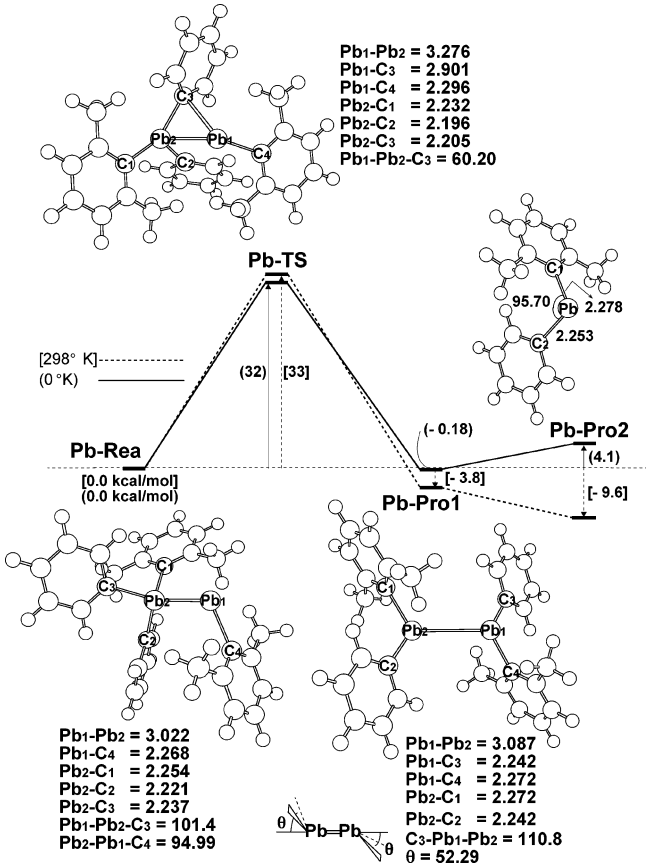

Figure 6. B3LYP/LANL2DZdp optimized geometries (in A and deg) and relative energies of ArPh2Pb·PbAr (Pb·Rea), transition state (Pb·TS), ArPhPb═PbPhAr (Pb·Pro1), and ArPhPb (Pb·Pro2) at 0 and 298 K.

in Table 1, our B3LYP computational results emphasize that symmetric Ar′PhE═EPhAr′ (**III**) is more stable than unsymmetrical Ar′Ph_2E−EAr′ (II) by 95, 13, and 0.18 kcal/mol for E = C, Si, and Pb, respectively. In contrast, the unsymmetrical Ar′Ph_2Sn−SnAr′ molecule is calculated to be 0.10 and 4.0 kcal/mol more stable than its symmetric isomer, Ar′PhGe═GePhAr′ and Ar′PhSn═SnPhAr′, respectively.

The large energy difference favoring Ar′PhC═CPhAr′ over Ar′Ph_2C−CAr′ compared to that favoring Ar′PhE═EPhAr′ over Ar′Ph_2E−EAr′ (E = Si, Ge, and Pb) strongly implies that C is more reluctant to form an unsymmetrical single bonded structure (**II**) than a symmetric double bonded species (**III**). On the other hand, our theoretical calculations suggest that both Ar′Ph_2E−EAr′ (II) and Ar′PhE═EPhAr′ (**III**) are nearly thermoneutral with an energy difference less than 4.0 kcal/mol for E = Ge, Sn, and Pb. We shall discuss these phenomena further after considering the TS between them in a later section.

The Ar′PhE═EPhAr′ (E = C, Si, Ge, Sn, and Pb) Product. The five sets of symmetric dimetallene products, Ar′PhE═EPhAr′ (**Pro1**), studied in this work are shown in Figures 2−6: **C**−**Pro1** (Ar′PhC═CPhAr′), **Si**−**Pro1** (Ar′PhSi═SiPhAr′), **Ge**−**Pro1** (Ar′PhGe═GePhAr′), **Sn**−**Pro1** (Ar′PhSn═SnPhAr′), and **Pb**−**Pro1** (Ar′PhPb═PbPhAr′), respectively. Cartesian coordinates calculated for the stationary points at the B3LYP/LANL2DZdp level are available as Supporting Information. It is well-known that the heavier analogues of olefins (R_2E═ER_2) do not exhibit classical planar geometry, but rather have a trans-bent structure (**III**), with pyramidalization of both R_2E groups. In fact, these compounds, containing so-called "nonclassical double bonds", have been proven to be the local minima on the potential energy surface for all the heavier analogues of ethylene. There is currently much discussion concerning these results in the literature.[1−5,25] Interested readers can find excellent reviews in ref 1−5.

TABLE 1: Energies (in kcal/mol) of Stationary Points Relative to the Reactants (Ar′Ph_2E.EAr′), Where E = C, Si, Ge, Sn, and Pb, at *T* = 0 K and All Are at the B3LYP/LANL2DZdp Level of Theory

system	Ar′Ph2E···EAr′ (Rea)	TS	Ar′PhE═EPhAr′ (Pro1)	Ar′PhE (Pro2)
E = C	0.0	63.9	−94.8	+32.8
E = Si	0.0	+60.5	−13.3	+38.5
E = Ge	0.0	+43.7	−3.38	+23.6
E = Sn	0.0	+35.3	+4.01	+18.3
E = Pb	0.0	+31.6	−0.181	+4.14

These double-bonded species contain no imaginary frequency at the level of theory used in our computational approach and, in turn, can be considered as true minima on the B3LYP potential energy surfaces. Unfortunately, as we have mentioned earlier, because of a lack of experimental and theoretical data on such double-bonded R′RE═ERR′ (**III**) species, the geometrical values presented in this work should be considered as predictions for future investigations. As demonstrated in Figures 2−6, the E═E bond length in the symmetric Ar′PhE═EPhAr′ (**III**) molecule was calculated to be in the order 1.367 Å (C−C) < 2.136 Å (Si−Si) < 2.354 Å (Ge−Ge) < 2.814 Å (Sn−Sn) < 3.087 Å (Pb−Pb), correlating with the atomic size of the main group 14 element E as it changes from C to Pb. Moreover, our DFT results reported that the greater the atomic number of the main group 14 element, also the greater the

pyramidalization angle θ (or out-of-plane angle). For instance, the pyramidalization angle θ increases in the order 0.82° (**C**−**Pro1**) < 1.2° (**Si**−**Pro1**) < 36° (**Ge**−**Pro1**) < 48° (**Sn**−**Pro1**) < 52° (**Pb**−**Pro1**). Again, the pyramidalization angles in **Sn**−**Pro1** and **Pb**−**Pro1** are far away from 0° (planar), and provide evidence for the corelike nature of the 5s and 6s electrons, that is, the so-called "inert s-pair effect",[24] discussed earlier. Apparently, the heavier main group 14 elements are pivotal atoms in this regard. These results are consistent with those reported in the previous studies cited above, and will not be discussed further.

Also, we have calculated the TSs for the 1,2-Ph shift in the Ar′Ph_2E−EAr′ (**II**) → Ar′PhE═EPhAr′ (**III**) process. All the transition states at the B3LYP level of theory are confirmed by calculation of the energy Hessian which shows only one imaginary vibrational frequency: 359i cm^{-1} (**C**−**TS**), 215i cm^{-1} (**Si**−**TS**), 139i cm^{-1} (**Ge**−**TS**), 82.4i cm^{-1} (**Sn**−**TS**), and 162i cm^{-1} (**Pb**−**TS**). It is noted that the primary similarity among these transition states is a three-center pattern involving carbon and the two main group 14 atoms (E). In addition, as shown in Table 1, our results suggest that the activation energy for such a 1,2-Ph shift decreases in the order (in kcal/mol) 63.9 (C) > 60.5 (Si) > 43.7 (Ge) > 35.3 (Sn) > 31.6 (Pb). Namely, the greater the atomic weight of the central atom E, the smaller the barrier height, and the easier the 1,2-Ph migration occurs. On the other hand, considering the reverse process (i.e., Ar′PhE═EPhAr′ (**III**) → Ar′Ph_2E−EAr′ (**II**)), the activation energies obtained at the B3LYP/LANL2DZ level are 158.7, 73.8, 47.1, 31.3, and 31.8 kcal/mol, respectively. All these energetic features strongly imply that there is a deep true minimum at Ar′PhC═CPhAr′, a structure stabilized by the very strong $p_\pi-p_\pi$ electronic delocalization. On the contrary, since the activation barriers for tin and lead are relatively small, 1,2-Ph migration should occur readily once the temperature is raised. As a result, when the temperature is increased, an equilibrium should exist between Ar′Ph_2E−EAr′ (**II**) and Ar′PhE═EPhAr′ (**III**) for E = Sn or Pb (vide infra).

Besides these, as mentioned earlier, a relatively small distance (1.536 Å) between central carbon atoms in the Ar′Ph_2C−CAr′ reactant may lead to steric crowding of the large alkyl groups during the 1,2-shift reaction. This would result in a larger than expected activation barrier for the C system. On the other hand, a large distance between the E atoms (in particular, 2.942 or 3.022Å for E = Sn or Pb) would reduce the crowding and, in turn, result in a lower barrier height. Furthermore, for the predicted transition-state structures (see Figures 2−6), DFT calculated the E_1-E_2 bond is stretched by 54%, 41%, 30%, 14%, and 8.4% for **C**−TS, **Si**−TS, **Ge**−TS, **Sn**−TS, and **Pb**−TS, respectively, relative to its value in the corresponding Ar′Ph_2E−EAr′ species. Also, it should be emphasized that the separating E_2-C_3 bond in **C**−TS, **Si**−TS, **Ge**−TS, **Sn**−TS, and **Pb**−TS is longer by 33%, 25%, 19%, 1.2%, and 0.63%, respectively, relative to that in the corresponding reactant. According to the Hammond's postulate,[27] these features suggest that Ar′Ph_2Sn−SnAr′ and Ar′Ph_2Pb−PbAr′ reach the TS relatively early, whereas Ar′Ph_2C−CAr′ arrives at the TS relatively late. That is to say, the barrier for the forward process is encountered earlier as the atomic weight of the central atom E becomes greater. One may thus anticipate a lower activation barrier for Ar′Ph_2Sn−SnAr′ and Ar′Ph_2Pb−PbAr′ than for Ar′Ph_2C−CAr′, which is confirmed by our B3LYP calculations as shown above.

In brief, our theoretical findings suggest that the symmetric double-bonded Ar′PhC═CPhAr′ (**III**) molecule is both kinetically and thermodynamically stable with respect to a 1,2-Ph shift. Conversely, the unsymmetrical single-bonded Ar′Ph_2E−EAr′ (**II**) compound containing much heavier main group 14 elements, in particular where E = Sn or Pb, is only kinetically stable during the 1,2-Ph migration reaction. Moreover, our model calculations have shown that the symmetric double-bonded dimer (Ar′PhE═EPhAr′) is more thermodynamically stable than the unsymmetrical isomer (Ar′Ph_2E−EAr′) for all the main group 14 elements, except for the case of tin.

TABLE 2: Thermodynamic Properties (in kcal/mol) of Stationary Points Relative to the Reactants (ArPh2E·EAr), Where E = C, Si, Ge, Sn, and Pb, at T = 298.15 K and All Are at the B3LYP/LANL2DZdp Level of Theory

system	thermodyn param	Ar′Ph_2E−EAr′ (Rea)	TS	Ar′PhE═EPhAr′ (Pro1)	Ar′PhE (Pro2)
E = C	ΔH	0.0	64.6	−94.8	33.4
	$\Delta S \times 10^{-2}$	0.0	0.49	0.060	5.38
	ΔG	0.0	63.1	−94.9	17.4
E = Si	ΔH	0.0	60.5	−13.1	38.6
	$\Delta S \times 10^{-2}$	0.0	0.44	0.080	5.01
	ΔG	0.0	59.2	−15.5	23.7
E = Ge	ΔH	0.0	44.1	−2.69	24.1
	$\Delta S \times 10^{-2}$	0.0	0.41	1.23	5.56
	ΔG	0.0	42.9	−6.35	7.55
E = Sn	ΔH	0.0	34.7	4.34	17.9
	$\Delta S \times 10^{-2}$	0.0	−0.95	1.08	4.53
	ΔG	0.0	37.6	1.13	4.39
E = Pb	ΔH	0.0	31.5	0.784	4.18
	$\Delta S \times 10^{-2}$	0.0	−0.53	1.52	4.61
	ΔG	0.0	33.1	−3.76	−9.56

3. The Ar′—E—Ph (E = C, Si, Ge, Sn, and Pb) Product. The five sets of two-coordinated Ar′−E−Ph products (**Pro2**) studied in this work are shown schematically in Figures 2−6: **C**−**Pro2** (Ar′−C−Ph), **Si**−**Pro2** (Ar′−Si−Ph), **Si**−**Pro2** (Ar′−Si−Ph), **Ge**−**Pro2** (Ar′−Ge−Ph), **Sn**−**Pro2** (Ar′−Sn−Ph), and **Pb**−**Pro2** (Ar′−Pb−Ph), respectively. Their Cartesian coordinates are given in the Supporting Information.

The E−C distance and the bond angle ∠C−E-C of Ar′−E−Ph obtained from our DFT calculations and reported in Figures 2−6 are in the order **C**−**Pro2** (1.432 Å) < **Si**−**Pro2** (1.898 Å) < **Ge**−**Pro2** (2.005 Å) < **Sn**−**Pro2** (2.193 Å) < **Pb**−**Pro2** (2.266 Å), whereas **C**−**Pro2** (122.3°) > **Si**−**Pro2** (102.5°) > **Ge**−**Pro2** (100.2°) > **Sn**−**Pro2** (96.90°) > **Pb**−**Pro2** (95.70°). That is, the E−C bond length increases due to the increasing size of the central atom E from C down to Pb, while the ∠C−E−C bond angle decreases owing to an increase in the relativistic effect[24] on a heavier central atom.

One striking result observed in this work is the dissociation of double-bonded Ar′PhE═EPhAr′ (**Pro1**) into two Ar′−E−Ph (**Pro2**) monomers, from which one may estimate the intrinsic $\sigma+\pi$ E═E bond energy.[28] According to our B3LYP results given in Table 1, the approximate values obtained for $E_{\sigma+\pi}$ (kcal/mol) are as follows: 128 (C═C), 52 (Si═Si), 28 (Ge═Ge), 14 (Sn═Sn), and 4.3 (Pb═Pb). Namely, these binding energies decrease regularly from silicon to lead, while that of carbon is much larger.[6,28] From the above analysis, it is clear that the binding energy for the case of the C═C bond is very strong, whereas those for the Ge═Ge, Sn═Sn, and Pb═Pb bonds are relatively weak, and the order of the E═E interaction is C ≫ Si > Ge > Sn > Pb. As a result, our theoretical conclusions support many experimental observations.[8,11]

Also, we have calculated the free energy differences (ΔG) for eq 3 at 298 K, which are given in Table 2 and Figures 2−6. As shown here the values of $\Delta\Delta G$ (kcal/mol) between **Pro1** and **Pro2** are 112, 39, 14, 3.3, and −5.8 for carbon, silicon, germanium, tin, and lead, respectively. Again, these results suggest that carbon derivatives having E═E bonded dimeric

structures are both kinetically and thermodynamically stable with respect to isomerization and dissociation. In contrast to the carbon compounds, the theoretical results report that, after considering the thermodynamic factors, the total energy of the two separated Ar′−Pb−Ph (**Pb**−**Pro2**) is below that of the double-bonded Ar′PhPb═PbPhAr′ (**Pb**−**Pro1**) species by 5.8 kcal/mol. The reason for this is that, as can be seen in Table 2, both a smaller enthalpy (ΔH) and a lager entropy (ΔS) favors the dissociated Ar′−Pb−Ph products to a large extent at 298 K. Accordingly, our theoretical investigations strongly suggest that, if the temperature is above room temperature (298 K), unsymmetrical Ar′Ph_2Sn−SnAr′ should be in equilibrium with monomeric Ar′−Sn−Ph, while Ar′Ph_2Pb−PbAr′ would readily dissociate into the two Ar′−Pb−Ph monomers. Indeed, our theoretical conclusions are in good agreement with the available experimental observations[8−10] as stated in the Introduction.

IV. Conclusion

Taking all of the aforementioned five reactions (eq 3: E = C, Sn, Ge, Sn, and Pb) studied in this paper, one can draw the following conclusions.

(1) In the case of carbon, owing to the very strong $p_\pi-p_\pi$ electronic delocalization in the planar C═C double bond system, the symmetric $R_2C{=}CR_2$ molecule will neither dissociate into monomers nor undergo 1,2-shift to other isomers. That is, the $R_2C{=}CR_2$ molecule should be both kinetically and thermodynamically stable toward isomerization and dissociation. This, in turn, makes $R_2C{=}CR_2$ the only structure existing in gas phase at all temperatures.

(2) In the case of silicon, if in the dimeric $R_2Si{=}SiR_2$ species, the R groups are bulky, then it would be expected to display a nearly planar structure due to the steric effects, which, in turn, would lead to stronger $p_\pi-p_\pi$ electronic interactions. As a result, such a double-bonded $R_2Si{=}SiR_2$ molecule will be stable kinetically and thermodynamically, and undergo neither dissociation nor intramolecular migration.

(3) In the case of germanium, the dimeric $R_2Ge{=}GeR_2$ species adopts a trans-bent structure, which results in weaker $p_\pi-p_\pi$ electronic delocalization. Moreover, the symmetric $R_2Ge{=}GeR_2$ molecule is calculated to be energetically thermoneutral with its unsymmetrical isomer, $R_3Ge-GeR$. Accordingly, the germanium system will adopt either $R_3Ge-GeR$ or $R_2Ge{=}GeR_2$ structure at low, and the monomeric R_2Ge structure at high temperature, respectively.

(4) In the case of tin, the unsymmetrical $R_3Sn-SnR$ species is estimated to be slightly more stable than its symmetric isomer, $R_2Sn{=}SnR_2$, and a high energy barrier exists between them. Therefore, $R_3Sn-SnR$ is more stable than $R_2Sn{=}SnR_2$ from both thermodynamic and kinetic viewpoints. In particular, if the size of one of the substituents is small (such as the Ph group in Ar′Ph_2Sn−SnAr′), then the unsymmetrical single-bonded $R_3Sn-SnR$ molecule will exist at low temperature. Because of the small energy difference between dimeric $R_2Sn{=}SnR_2$ and monomeric R_2Sn, the unsymmetrical $R_3Sn-SnR$ species will be in equilibrium with its R_2Sn monomers at high temperature.

(5) In the case of lead, the unsymmetrical $R_3Pb-PbR$ species is predicted to be nearly thermoneutral with its symmetric isomer, $R_2Pb{=}PbR_2$, the former being less stable than the latter by only 0.2 kcal/mol. In addition, the barrier height between these two molecules is estimated to be at least 30 kcal/mol. In consequence, our theoretical results predict that, from a kinetic viewpoint, the unsymmetrical $R_3Pb-PbR$ compound should exist at low temperature. On the other hand, since the total energy of the two separated R_2Pb monomers is calculated to be lower than that of the symmetric $R_2Pb{=}PbR_2$ dimer, it is reasonable to predict that both unsymmetrical $R_3Pb-PbR$ and symmetric $R_2Pb{=}PbR_2$ species will spontaneously dissociate into R_2Pb monomers at room temperature.

(6) This work has demonstrated that it is the nature of the group 14 element, its organic substituents, the stability of the bonding scheme, as well as the strength of the E−E (E = C, Si, Ge, Sn, and Pb) interaction that play crucial roles in the type of product obtained.

We encourage experimentalists to design new experiments to confirm our predictions.

Acknowledgment. We are thankful to the National Center for High-Performance Computing of Taiwan for generous amounts of computing time. We also thank the National Science Council of Taiwan for their financial support. Special thanks are also due to the reviewers for very helpful suggestions and comments.

Supporting Information Available: Cartesian coordinates calculated for the stationary points at the B3LYP/LANL2DZdp level. This material is available free of charge via the Internet at http://pubs.acs.org.

References and Notes

(1) For disilenes, see: (a) West, R. *Pure Appl. Chem.* **1984**, *56*, 163. (b) Raabe, G.; Michl, J. *Chem. Rev.* **1985**, *85*, 419. (c) Cowley, A. H.; Norman, N. C. *Prog. Inorg. Chem.* **1986**, *34*, 1. (d) West, R. *Angew. Chem., Int. Ed. Engl.* **1987**, *26*, 1201. (e) Raabe, G.; Michl, J. In *The Chemistry of Organic Silicon Compound*; Patai, S., Rappoport, Z., Eds.; Wiley: New York, 1989. Part 2; Chapter 17. (f) Tsumuraya, T.; Batcheller, S. A.; Masamune, S. *Angew. Chem., Int. Ed. Engl.* **1991**, *30*, 902. (g) Weidenbruch, M. *Coord. Chem. Rev.* **1994**, *130*, 275. (i) Okazaki, R.; West, R. *Adv. Organomet. Chem.* **1996**, *39*, 231. (j) Iwamoto, T.; Sakurai, H.; Kira, M. *Bull. Chem. Soc. Jpn.* **1998**, *71*, 2741. (k) Gaspar, P. P.; West, R. *The Chemistry of Organic Silicon Compounds*; Rappoport, Z., Apeloig, Y., Eds. John Wiley & Sons: New York, 1998; Vol. 2, Part 3; Chapter 43.

(2) For digermenes, see: (a) Hitchcock, P. B.; Lappert, M. F.; Miles, S. J.; Thorne, A. J. *J. Chem. Soc Chem. Commun.* **1984**, 480. (b) Escudie, J.; Couret, C.; Ranaivonjatovo, H.; Satge, J. *Coord. Chem. Rev.* **1994**, *130*, 427 and references therein (c) Baines, K. M.; Stibbs, W. G. *Adv. Organomet. Chem.* **1996**, *39*, 275. (d) Escudie, J.; Ranaivonjatovo, H. *Adv. Organomet. Chem.* **1999**, *44*, 113. (e) Weidenbruch, M. *J. Organomet. Chem.* **2002**, *646*, 39.

(3) For distannenes, see: (a) Davidson, P. J.; Lappert, M. F. *J. Chem. Soc. Chem. Commun.* **1973**, 317. (b) Goldberg, D. E.; Harris, D. H.; Lappert, M. F.; Thomas, K. M. *J. Chem.* Soc., Chem. Commun. **1976**, 261. (c) Gruetzmacher, H.; Pritzkow, H.; Edelmann, F. T. *Organometallics*, **1991**, *10*, 23. (d) Layh, U.; Pritzkow, H.; Gruetzmacher, H. *J. Chem.* Soc., Chem. Commun. **1992**, 260. (e) Weidenbruch, M.; Kilian, H.; Peters, K.; von Schnering, H. G.; Marsmann, H. *Chem. Ber.* **1995**, *128*, 983.

(4) For diplumbenes, see: (a) Klinkhammer, K. W.; Fassler, T. F.; Gruetzmacher, H. *Angew. Chem. Int. Ed. Engl.* **1998**, *37*, 124. (b) Sturmann, M.; Weidenbruch, M.; Klinkhammer, K. W.; Lissner, F.; Marsmann, H. *Organometallics* **1998**, *17*, 4425. (c) Weidenbruch, M. *Eur. J. Inorg. Chem.* **1999**, 373. (d) Sturmann, M.; Saak, W.; Marsmann, H.; Weidenbruch, M. *Angew. Chem., Int. Ed. Engl.* **1999**, *38*, 187. (e) Wang, X.; Andrews, L. *J. Am. Chem. Soc.* **2003**, *125*, 6581.

(5) For recent reviews, see: (a) Grev, R. S. *Adv. Organomet. Chem.* **1991**, *33*, 125. (b) Esoudie, J.; Couret, C.; Ranaivonjatovo, H.; Satge, J. *Coord. Chem. Rev.* **1994**, *94*, 427. (c) Driess, M. *Coord. Chem. Rev.* **1995**, *145*, 1. (d) Mackay, K. M. in *The Chemistry of Organic Germanium, Tin, and Lead Compounds*; Patai, S., Ed.; Wiley: Chichester, U.K., 1995; Chapter 4. (e) Klinkhammer, K. W. *Angew. Chem., Int. Ed. Engl.* **1997**, *36*, 2320. (f) Barrau, J.; Rina, G. *Coord. Chem. Rev.* **1998**, *178*, 593. (g) Power, P. P. *J. Chem.* Soc. Dalton Trans. **1998**, 2939. (h) (i) Tokitoh, N.; Matsumoto, T.; Okazaki, R. *Bull.* Chem. Soc. Jpn. **1999**, *72*, 1665. (i) Robinson, G. H. *Acc. Chem. Res.* **1999**, *32*, 773. (j) Power, P. P. *Chem. Rev.* **1999**, *99*, 3463. (k) Leigh, W. J. *Pure Appl. Chem.* **1999**, *71*, 453. (l) Tokitoh, N. *Pure Appl. Chem.* **1999**, *71*, 495. (m) Gruetzmacher, H.; Fassler, T. F. *Chem.—Eur. J.* **2000**, *6*, 2317. (n) Kira, M.; Iwamoto, T. *J. Organomet. Chem.* **2000**, *610*, 236. (o) Tokitoh, N.; Okazaki, R. *Coord. Chem. Rev.* **2000**, *210*, 251. (p) Malcolm, N. O. J.; Gillespie, R. J.; Popelier, P. L. A. *J. Chem. Soc., Dalton Trans.* **2002**, 3333. (q) Tokitoh, N.; Okazaki, R. *The Chemistry of Organic Germanium, Tin and Lead Compounds*; Rappoport, Z., Ed.; Wiley: Chichester, U.K., 2002; Vol. 2, Chapter 13. (r) Klinkham-

mer, K. W. *The Chemistry of Organic Germanium, Tin and Lead Compounds*, Rappoport, Z., Ed.; Wiley: Chichester, U.K., 20002; Vol. 2; Chapter 4. (s) Lee, V. Y.; Sekiguchi, A. *Organometallics* **2004**, *23*, 2822. (t) Schleyer, P. v. R. *The Chemistry of Organic* Silcon *Compounds*; Rappoport, Z.; Apeloig, Y. Ed.; John Wiley & Sons: London, 2001; pp 1−163 and references therein.

(6) (a) Trinquier, G. *J. Am. Chem. Soc.* **1990**, *112*, 2130. (b) Trinquier, G. *J. Am. Chem. Soc.* **1991**, *113*, 144.

(7) It was reported that, for instance, the greater bridging tendency of hydrogen versus alkyl or aryl can be found in group 13 element derivatives of elements such as boron or gallium. See: Greenwood, N. N.; Earnshaw, A. *A Chemistry of Elements*, 2nd ed.; Butterworth-Heinemann: Woburn, MA, 1997; p 65.

(8) Phillips, A. D.; Hino, S.; Power, P. P. *J. Am. Chem. Soc.* **2003**, *125*, 7520.

(9) Stender, M.; Pu, L.; Power, P. P. *Organometallics* **2001**, *20*, 1820.

(10) Pu, L.; Power, P. P.; Boltes, I.; Herbst-Irmer, R. *Organometallics* **2000**, *19*, 352.

(11) The NMR spectroscopy has shown that the structure of the dimers shown in eq 2 is symmetric: that is, each E center is spectroscopically equivalent. See: (a) Tokitoh, N.; Suzuki, H.; Okazaki, R. *J. Am. Chem. Soc.* **1993**, *115*, 10428. (b) Bona, M. A.; Cassani, M. C.; Keates, J. M.; Lawless, G. A.; Lappert, M. F.; Sturmann, M.; Weidenbruch, M. *Dalton Trans.* **1998**, 1187. (c) Kishikawa, K.; Tokitoh, N.; Okazaki, R. *Chem. Lett.* **1998**, 239. (d) Zilm, K. W.; Lawless, G. A.; Merrill, R. M.; Miller, J. M.; Webb, G. G. *J. Am.* Chem. Soc. **1987**, *109*, 7236.

(12) Simons, R. S.; Pu, L.; Olmstead, M. M.; Power, P. P. *Organometallics* **1997**, *16*, 1920.

(13) Although it would be desirable to carry out complete calculations for the systems that were studied experimentally (i.e., the Ar* ligand), we have therefore used a simplified model, in which the bulky Ar* were replaced with the smaller Ar′ ligands.

(14) (a) Becke, A. D. *Phys. Rev. A*, **1988**, *38*, 3098. (b) Becke, A. D. *J. Chem. Phys.* **1993**, *98*, 5648.

(15) Lee, C.; Yang, W.; Parr, R. G. *Phys. Rev. B*, **1988**, *37*, 785.

(16) (a) Dunning, T. H., Jr.; Hay, P. J. In *Modern Theoretical Chemistry*, Schaefer, H. F., III, Ed.; Plenum: New York, 1976; pp 1−28. (b) Hay, P. J.; Wadt, W. R. *J. Chem. Phys.* **1985**, *82*, 270. (c) Hay, P. J.; Wadt, W. R. **1985**, *82*, 284. (d) Hay, P. J.; Wadt, W. R. **1985**, *82*, 299.

(17) Check, C. E.; Faust, T. O.; Bailey, J. M.; Wright, B. J.; Gilbert, T. M.; Sunderlin, L. S. *J. Phys. Chem. A* **2001**, *105*, 8111.

(18) Gaussian 03, Revision C. 02: Frisch, M. J.; Trucks, G. W.; Schlegel, H. B.; Scuseria, G. E.; Robb, M. A.; Cheeseman, J. R.; Zakrzewski, V. G.; Montgomery, J. A., Jr.; Vreven, T.; Kudin, K. N.; Burant, J. C.; Millam, J. M.; Iyengar, S. S.; Tomasi, J.; Barone, V.; Mennucci, B.; Cossi, M.; Scalmani, G.; Rega, N.; Petersson, G. A.; Nakatsuji, H.; Hada, M.; Ehara, M.; Toyota, K.; Fukuda, R.; Hasegawa, J.; Ishida, M.; Nakajima, T.; Honda, Y.; Kitao, O.; Nakai, H.; Klene, M.; Li, X.; Knox, J. E.; Hratchian, H. P.; Cross, J. B.; Adamo, C.; Jaramillo, J.; Gomperts, R.; Stratmann, R. E.; Yazyev, O.; Austin, A. J.; Cammi, R.; Pomelli, C.; Ochterski, J. W.; Ayala, P. Y.; Morokuma, K.; Voth, G. A.; Salvador, P.; Dannenberg, J. J.; Zakrzewski, V. G.; Dapprich, S.; Daniels, A. D.; Strain, M. C.; Farkas, O.; Malick, D. K.; Rabuck, A. D.; Raghavachari, K.; Foresman, J. B.; Ortiz, J. V.; Cui, Q.; Baboul, A. G.; Clifford, S.; Cioslowski, J.; Stefanov, B. B.; Liu, G.; Liashenko, A.; Piskorz, P.; Komaromi, I.; Martin, R. L.; Fox, D. J.; Keith, T.; Al-Laham, M. A.; Peng, C. Y.; Nanayakkara, A.; Challacombe, M.; Gill, P. M. W.; Johnson, B.; Chen, W.; Wong, M. W.; Gonzalez, C.; Pople, J. A. Gaussian, Inc.: Wallingford CT, 2003.

(19) Eichler, B. E.; Power, P. P. *Inorg. Chem.* **2000**, *39*, 5444.

(20) However, it was shown that singlet methylmethylene (H_3C-CH) is the transition state for hydrogen scrambling in ethylene and lies high in energy at 70−80 kcal/mol above ethylene. See ref 6a.

(21) One referee pointed out that singly bridged forms are possible stable forms, but are only considered as transition states in this work. In order to answer this question, we reexamined the B3LYP/LANL2DZdp calculations focusing on the singly bridged isomers containing group 14 elements. Despite considerable effort, no local minimum could be found. The reason for this is presumably that singly bridged isomers reported by Power and Trinquier have just one bridged atom, rather than a bulky group. As a result, owing to the steric effect, singly bridged forms studied in this work are predicted to be transition states. Also see: (a) Stanciu, C.; Richards, A. F.; Power, P. P. *J. Am. Chem. Soc.* **2004**, *126*, 4106. (b) ref 6.

(22) (a) Rice, J. C.; Handy, N. C. *Chem. Phys. Lett.* **1984**, *107*, 365. (b) Balasubramanian, K.; McLean, A. D. *J. Chem. Phys.* **1986**, *85*, 5117. (c) Karolczak, J.; Harper, W. W.; Grev, R. S.; Clouthier, D. J. *J. Chem. Phys.* **1995**, *103*, 2839. (d) Su, M.-D. *J. Phys. Chem. A* **2002**, *106*, 9563.

(23) Kaupp, M.; Schleyer, P. v. R. *J. Am. Chem. Soc.* **1993**, *115*, 1061.

(24) (a) Pyykkö. P.; Desclaux, J.-P. *Acc. Chem. Res.*, **1979**, *12*, 276. (b) Kutzelnigg, W. *Angew*. Chem., Int. Ed. Engl. **1984**, *23*, 272. (c) Pyykkö. P. *Chem. Rev.*, **1997**, *97*, 597.

(25) It was reported that the Sn═Sn double bond is composed of two relatively weak polar-dative interactions, in comparison to the relatively strong (usually ca. 40 kcal/mol) Sn−Sn covalent single bond. See: (a) Lappert, M. F. *Adv. Chem. Ser.* **1976**, *No. 150*, 256. (b) Simoes, J. A. M.; Liebman, J. F.; Slayden, S. W. In *The Chemistry of Organic Germanium, Tin, and Lead Compounds*; Patai, S., Ed.; Wiley: Chichester, U.K., 1995; Chapter 4.

(26) For instance, see: Liang, C.; Allen, C. C. *J. Am. Chem. Soc.*, **1990**, *112*, 1039. (b) Karni, M.; Apeloig, Y. *J. Am. Chem. Soc.*, **1990**, *112*, 8589. (c) Escudié, J.; Couret, C.; Ranaivonjatovo, H. *Coord. Chem. Rev.* **1998**, *178*, 565.

(27) Hammond, G. S. *J. Am. Chem. Soc.* **1954**, *77*, 334.

(28) The natural dissociation product of the planar double bond $R_2E═ER_2$ is a pair of $^3B_1$ triplet R_2E: species. The natural dissociation product of a trans-bent double bond is a pair of $^1A_1$ singlet R_2E species. To make easier to analyze and to interpret, the energy of the two separated singlet R_2E fragments is chosen in this work. See: (a) Reference 6; (b) Chen, W.-C.; Su, M.-D.; Chu, S.-Y. *Organometallics* **2001**, *20*, 564 and references therein.